Available online at www.sciencedirect.com
SCIENCE DIRECT
Microporous and Mesoporous Materials 92 (2006) 64–70
MICROPOROUS AND MESOPOROUS MATERIALS
www.elsevier.com/locate/micromeso

Granular and monolithic activated carbons from KOH-activation of olive stones

Ruth Ubago-Pérez, Francisco Carrasco-Marín, David Fairén-Jiménez, Carlos Moreno-Castilla *

Departamento de Química Inorgánica, Facultad de Ciencias, Universidad de Granada, 18071 Granada, Spain

Received 1 October 2005; received in revised form 23 December 2005; accepted 3 January 2006
Available online 17 February 2006

Abstract

Different activated carbons were prepared by KOH-activation of carbonized olive stones by varying the KOH/carbon weight ratio and the particle size of the precursor. The activated carbon with the best surface characteristics was furthermore steam-activated. Other activated carbon was obtained by using directly olive stones as raw material. In this case the precursor particles were broken by the KOH solution, obtaining an activated carbon with an extremely fine particle size. Different monoliths were prepared from this powder activated carbon by using a binder and pressure. All samples were characterized by N_2 and CO_2 adsorption at −196 and 0 °C, respectively, and scanning electron microscopy. Some samples were also characterized by benzene adsorption at 30 °C. Carbon monoliths were used to remove toluene from a toluene/air flow under dynamic conditions. Column bed characteristics were obtained from breakthrough curves. Amounts adsorbed at saturation were much higher than others reported in the literature and that were obtained by using different activated carbons.

Keywords: KOH-activation; Activated carbons; Monolithic activated carbons; Toluene removal

1. Introduction

Chemical activation with KOH of lignocellulosic materials and coals is one of the known preparation methods of activated carbons [1–10]. This method has received a growing interest in the last years [11–20], mainly addressed to elucidate the mechanism of activation. It permits the one-step preparation of activated carbons with a well-developed microporosity and a high surface area.

Previous results found in our laboratory [11] showed that chemical activation of olive-mill waste water with KOH produced activated carbons (ACs) with much lower ash content, higher nitrogen surface area and much better developed porosity than in the case of chemical activation with phosphoric acid or physical activation with CO_2 at 840 °C.

The main objective of this work is to prepare activated carbons from olive stones by chemical activation with KOH. This method can produce granular or powder activated carbons with varying surface properties depending on the experimental procedure. The present work also explores the possibility to obtain activated carbon monoliths by pressing powder activated carbons mixed with a binder. Activated carbon monoliths are of great importance in different areas such as gas storage [21], volatile organic compounds removal [22] and catalysis [23].

2. Experimental

2.1. Preparation of activated carbons

ACs were prepared from olive stones by chemical activation with KOH. The raw material was firstly ground and sieved to a size range between 1 and 2 mm. After that, it was carbonized at 840 °C for 1 h in a N_2 flow

* Corresponding author. Tel.: +34 958 243 323; fax: +34 958 248 526.
E-mail address: cmoreno@ugr.es (C. Moreno-Castilla).

1387-1811/$ - see front matter © 2006 Elsevier Inc. All rights reserved.
doi:10.1016/j.micromeso.2006.01.002

(300 cm^3/min), with a heating rate of 10 °C/min. Weight loss during the carbonization process was 76%. The carbonized sample was demineralised by alternative treatment with HCl and HF, following the method described elsewhere [24].

The demineralised carbon was again sieved to a particle size range between 1 and 1.4 mm. Different portions of this carbon were impregnated with an aqueous solution of KOH, as described elsewhere [11] to yield four samples with KOH/carbon weight ratios of 1/1, 2/1, 4/1 and 5/1. Suspensions were heated at 60 °C for 12 h and then heated at 110 °C to dryness. Posteriorly, these samples were pyrolised at 300 °C for 3 h and finally to 800 °C for 2 h in N_2 flow (300 cm^3/min). The heating rate was 10 °C/min. These ACs will be referred to in the text as A1, A2, A4 and A5, which correspond with the KOH/carbon weight ratios of 1/1, 2/1, 4/1 and 5/1, respectively.

Other two ACs were prepared following the same recipe than carbon A2, but from different particle size range in the demineralised carbonized sample. Thus, activated carbons B and C were obtained from particle size ranges between 0.63 and 0.80 mm and 0.08 and 0.15 mm, respectively. Activated carbon B was further steam-activated at 800 °C up to a 22% burn-off, following the method described elsewhere [25]. This sample will be referred to in the text as BW.

Finally, another AC, sample H, was obtained by chemical activation of the original raw material, olive stone. For this purpose, the raw material with a particle size range between 1 and 2 mm was impregnated with an aqueous solution of KOH to yield a KOH/olive stone ratio of 2/1. Activation method was similar as the above commented for A2 sample. It is noteworthy that the precursor grains were broken during the impregnation giving place to a finely divided material. This ensures the homogeneity of the mixture between the raw material and the activating reagent [17].

All AC samples were washed with 0.1 N HCl and then with distilled water till absence of chloride ions in the washing waters. Preparation conditions of the different activated carbons used are summarized in Table 1.

Table 1
Preparation conditions of carbon materials used

Sample	Raw material	Particle size (mm)	KOH/carbon weight ratio	Carbonization temperature (°C)–gas flow
Carbonized	Olive stones	1–2	–	840–N_2
A1	Carbonized	1–1.4	1/1	840–N_2
A2	Carbonized	1–1.4	2/1	840–N_2
A4	Carbonized	1–1.4	4/1	840–N_2
A5	Carbonized	1–1.4	5/1	840–N_2
B	Carbonized	0.63–0.80	2/1	840–N_2
C	Carbonized	0.08–0.15	2/1	840–N_2
BW	B	–	–	800–H_2O
H	Olive stones	1–2	2/1	800–N_2

Sample H was used to prepare some monoliths. For this purpose, it was mixed with polyvinyl alcohol (PVA), which acted as a binder, at two different concentrations: 5 and 15 wt.%. The mixture was pressed at two different pressures, 5 and 10 bar, while heating at 200 °C for 45 min. The monoliths will be referred to in the text as H followed by two numbers, which indicate the pressure and the PVA percentage used, respectively.

2.2. Characterization of activated carbons

All activated carbons prepared were characterized by N_2 and CO_2 adsorption at −196 and 0 °C. Some selected samples were characterized also by benzene adsorption at 30 °C. Adsorption isotherms were measured in conventional volumetric (N_2 and CO_2) or gravimetric (benzene) equipments made in Pyrex glass and free of mercury and grease, which reached a dynamic vacuum of more than 10^{-6} mbar at the sample location. Equilibrium pressure was measured with a Baratron transducer from MKS. The gravimetric equipment had also quartz springs with a constant of approximately 0.25 mm/mg; the spring extension was measured with a cathetometer to a precision of 0.01 mm.

BET equation was applied to N_2 adsorption isotherms from which an apparent BET surface area, S_{BET}, was obtained, considering as 0.162 nm^2 the molecular area of N_2 at −196 °C [26]. Total pore volume, V_T, was obtained from N_2 adsorption isotherm at $p/p_0 = 0.95$ (Gurvitsch rule).

The Dubinin–Radushkevich (DR) equation was applied to the N_2, CO_2 and benzene isotherms to obtain the micropore volume accessible to these adsorptives, W_0, and the characteristic adsorption energy, E_0. Once known this value, the mean micropore width, L_0, was obtained by applying the Stoeckli equation [27] (Eq. (1))

$$L_0\ (\mathrm{nm}) = 10.8/(E_0 - 11.4\ \mathrm{kJ/mol}) \quad (1)$$

Liquid densities of N_2 at −196 °C, CO_2 at 0 °C and benzene at 30 °C were taken as 0.808, 1.023 and 0.877 g/cm^3 [26,28]. Affinity coefficients used in the DR equation for N_2, CO_2 and benzene were taken as 0.33, 0.31 and 1, respectively.

Some samples were analyzed by scanning electron microscopy (SEM) using a Karl Zeiss DSM 950 microscope. Images were obtained at an excitation energy of 20 kV.

2.3. Toluene adsorption

Some of the monoliths prepared were used to study the removal of toluene from a toluene/air mixture under dynamic conditions. The bed depth was 8 mm (0.1 g carbon) and its internal diameter 7 mm. Adsorption was carried out at 25 °C with a flow of 60 cm^3/min and a toluene concentration of 740 ppmv in a toluene/air mixture. Toluene concentration at the column bed outlet was

followed by gas chromatography. Samples were outgassed before the adsorption experiments by passing through the column bed a He flow of 60 cm^3/min at 200 °C for 2 h.

3. Results and discussion

N_2 adsorption isotherms obtained on samples A1–A5 are depicted, as an example, in Fig. 1. Benzene adsorption isotherms showed a similar shape to those of N_2, and they are of type I of the BDDT classification with a plateau practically parallel to the p/p_0-axis, indicating that these are essentially microporous samples with none or very low mesoporosity.

Variation of S_{BET} against KOH/carbon weight ratio used in chemical activation is depicted in Fig. 2, which shows that S_{BET} markedly increases up to a KOH/carbon weight ratio of 2/1. Above this weight ratio the increase in S_{BET} is not significant in comparison to the amount of activating reagent used. For this reason, the KOH/carbon weight ratio of 2/1 was chosen to prepare the other activated carbons B, C and H.

Results from DR equation applied to N_2, CO_2 and benzene are compiled in Table 2, together with the total pore volume V_T. Application of DR equation to adsorption isotherms obtained on A1 and A2 samples are depicted, as an example, in Figs. 3 and 4, respectively.

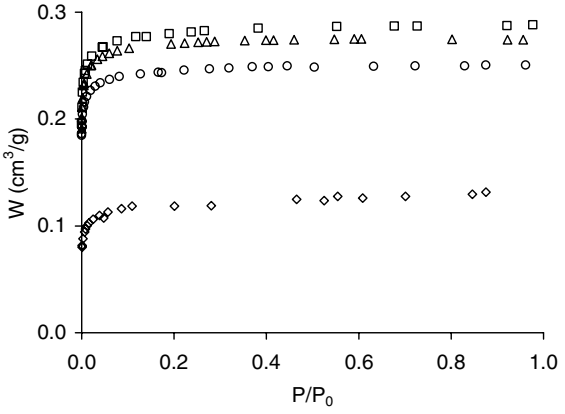

Fig. 1. N_2 adsorption isotherms at −196 °C on samples: (◊) A1; (○) A2; (△) A4; (□) A5.

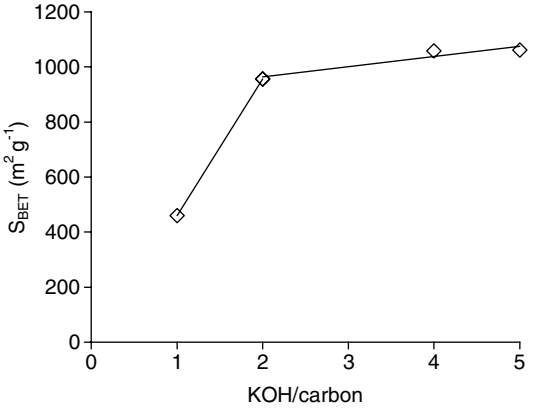

Fig. 2. Variation of S_{BET} against the KOH/carbon weight ratio.

Activated carbon A1 shows a $W_0(CO_2)$ value higher than its $W_0(N_2)$ and $W_0(C_6H_6)$ values and so, DR plots present two different straight lines one for CO_2 and another one for N_2 and benzene (Fig. 3). This is indicative of constrictions at the entrance of the micropores, which reduce the accessibility of N_2 and C_6H_6. In the case of N_2 due to the low adsorption temperature used (−196 °C), and in the case of C_6H_6 due to its greater minimal dimension (0.37 nm) than that of CO_2 (0.28 nm). Thus, Fig. 3 shows a characteristic curve for CO_2 and another one for N_2 and benzene.

The W_0 value obtained with the three adsorbates is very similar in the case of sample A2. This indicates that the increase in the KOH/carbon weight ratio eliminates the micropore constrictions. A2 sample shows an unique characteristic curve for N_2, CO_2 and benzene adsorption (Fig. 4). The micropore width of this sample is around 0.60 nm determined with the three adsorbates.

The increase in the KOH/carbon weight ratio to 4/1 and 5/1 (A4 and A5 samples) produces a slight increase in the micropore volume, W_0. The total pore volume, V_T, of these samples is equal or slightly greater than $W_0(N_2)$, which indicates that they are essentially microporous carbons. Similar negligible development of meso and macroporosity has been found before by other authors [17]. However, results found here are different from those obtained in carbons prepared by KOH-activation of olive-mill waste water [11], because these latter carbons developed a large micro, meso and macropore volumes. Finally, A4 and A5 samples show the same W_0 value determined from both N_2 and CO_2, as in the case of A2 sample, indicative of an homogeneous micropore size distribution.

Another variable that affects the surface characteristics of the activated carbons prepared by KOH-activation is the particle size of the raw material used. For this reason, two activated carbons (B and C) were prepared following the same recipe of activated carbon A2, but using two different particle size ranges. Results obtained are compiled in Table 3, which shows that B sample has a larger S_{BET} and micropore volume than A2. This is due to the higher surface of the small particles compared to that of the larger particles.

In addition, sample B has the $W_0(N_2)$ value slightly higher than the $W_0(CO_2)$ value indicative of a wider and heterogeneous micropore size distribution [26]. However, the use of a smaller particle size range in the carbonized raw material, sample C, gives place to a decrease in S_{BET} and micropore volume. In this last sample, the difference between V_T and $W_0(N_2)$ is the highest found, which indicates an incipient formation of mesopores. These results point out that C sample was more activated than B sample, due to the smaller particle size range used during the activation of the former. Therefore, there is an optimum particle size range in the carbonized raw material that yields

Table 2
Micropore volume, W_0, mean micropore width, L_0, and total pore volume, V_T, of different activated carbons

Sample	$W_0(N_2)$ (cm^3/g)	$W_0(CO_2)$ (cm^3/g)	$W_0(C_6H_6)$ (cm^3/g)	$L_0(N_2)$ (nm)	$L_0(CO_2)$ (nm)	$L_0(C_6H_6)$ (nm)	V_T (cm^3/g)
A1	0.19	0.28	0.17	1.42	0.56	1.11	0.21
A2	0.38	0.39	0.40	0.62	0.62	0.57	0.38
A4	0.40	0.39	–	0.57	0.63	–	0.42
A5	0.41	0.40	0.45	0.57	0.64	0.55	0.44

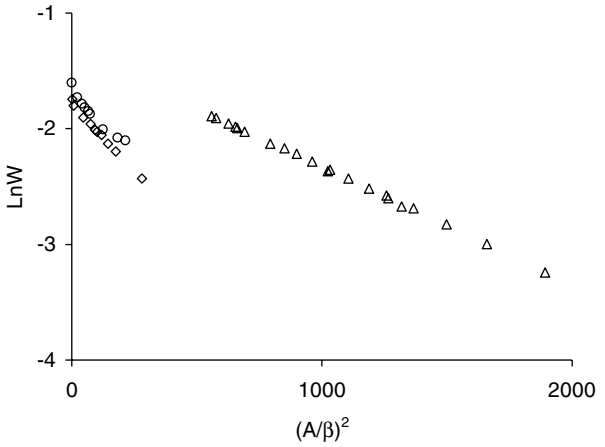

Fig. 3. Application of DR equation to the adsorption of: (◊) benzene; (○) N_2; (△) CO_2; on activated carbon A1.

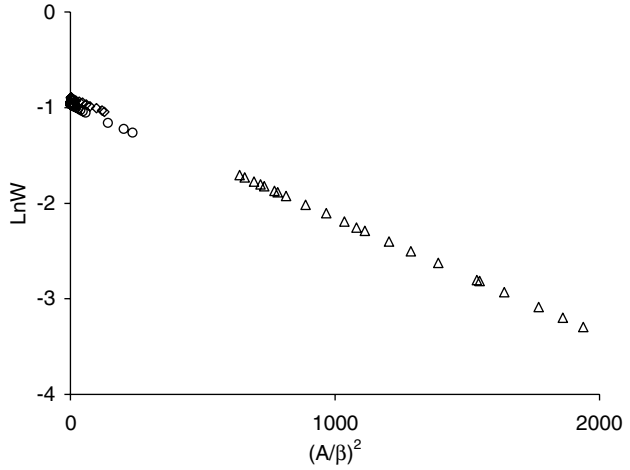

Fig. 4. Application of DR equation to the adsorption of: (◊) benzene; (○) N_2; (△) CO_2; on activated carbon A2.

activated carbon with the best microporosity and surface area characteristics.

Steam-activation of sample B yielded sample BW (Table 3). This produces an increase in S_{BET} and $W_0(N_2)$. In this case $W_0(N_2)$ is much greater than $W_0(CO_2)$ indicative of a very wide and heterogeneous micropore size distribution, and although $L_0(CO_2)$ in B and BW samples is very close, however $L_0(N_2)$ in BW sample is much greater than in B sample. Results obtained point out that during the steam-activation of B sample the narrow micropores are widened, giving a mean micropore width of 1.36 nm. In this case V_T is very similar to $W_0(N_2)$, so practically no mesoporosity was developed during steam-activation of B.

Heat-treatment of coals before their KOH-activation reduces considerably the ease of the reactions that take place during activation [15]. In the same way, it has been reported [17] that the interaction with the activating agent is more intensive for the non-carbonized material than for the char. These reasons have led us to prepare an activated carbon (H sample) directly from the original non-carbonized olive stones as raw material, following the same procedure used to prepare A2. Results obtained are compiled in Table 3. H sample shows a greater S_{BET}, $W_0(N_2)$ and V_T values than A2 sample. Furthermore, the $W_0(N_2)$ value of H is greater than its $W_0(CO_2)$ value, which as commented above indicates a wide and heterogeneous micropore size distribution. Therefore, the KOH-activation of the non-carbonized raw material produces a widening of the narrow micropores, which pass from 0.62 nm (A2) to 1.37 nm (H). This sample is also essentially microporous due to the small difference between $W_0(N_2)$ and V_T values.

A possible inconvenient for the practical use of sample H is that it is a very light material, due to the breaking of the precursor particles after their impregnation with the KOH solution. This is due to the fragmentation and solution of lignin and hemicellulose produced by the attack of strongly nucleophilic hydroxyl ions [17].

SEM micrographs of selected samples are shown in Fig. 5. The development of large macropores on the particle surface can be appreciated when going from the carbonized raw material to the activated carbons A2 and B. The SEM image of the H sample is very different to that of the other activated carbons. Thus, its appearance is an indication of the lightness of its particles.

To overcome the possible inconvenient in the practical use of H carbon, due to its extremely fine particle size, it was used to manufacture different monoliths, as indicated in Section 2. A photograph of the monoliths prepared is shown in Fig. 6.

Results from N_2 and CO_2 adsorption are compiled in Table 4. S_{BET} of the monoliths is smaller than that of H sample. An increase in the binder concentration from 5% to 15% has a negative effect in S_{BET} and micropore volumes. However, an increase in the pressure used to prepare the monoliths from 5 to 10 bar has a very slight positive effect on them. Thus, sample H-10-5 has the best surface characteristics. Similarly, samples prepared with the smallest binder concentration, H-5-5 and H-10-5, have a $W_0(CO_2)$ micropore volume similar to that of sample H

Table 3
BET surface area, micropore volume, W_0, mean micropore width, L_0, and total pore volume, V_T, of different activated carbons

Sample	S_{BET} (m^2/g)	$W_0(N_2)$ (cm^3/g)	$W_0(CO_2)$ (cm^3/g)	$L_0(N_2)$ (nm)	$L_0(CO_2)$ (nm)	V_T (cm^3/g)
A2	957	0.38	0.39	0.62	0.62	0.38
B	1243	0.49	0.44	0.65	0.64	0.53
C	1090	0.38	–	0.81	–	0.45
BW	1484	0.62	0.38	1.36	0.72	0.64
H	1310	0.54	0.33	1.37	0.62	0.58

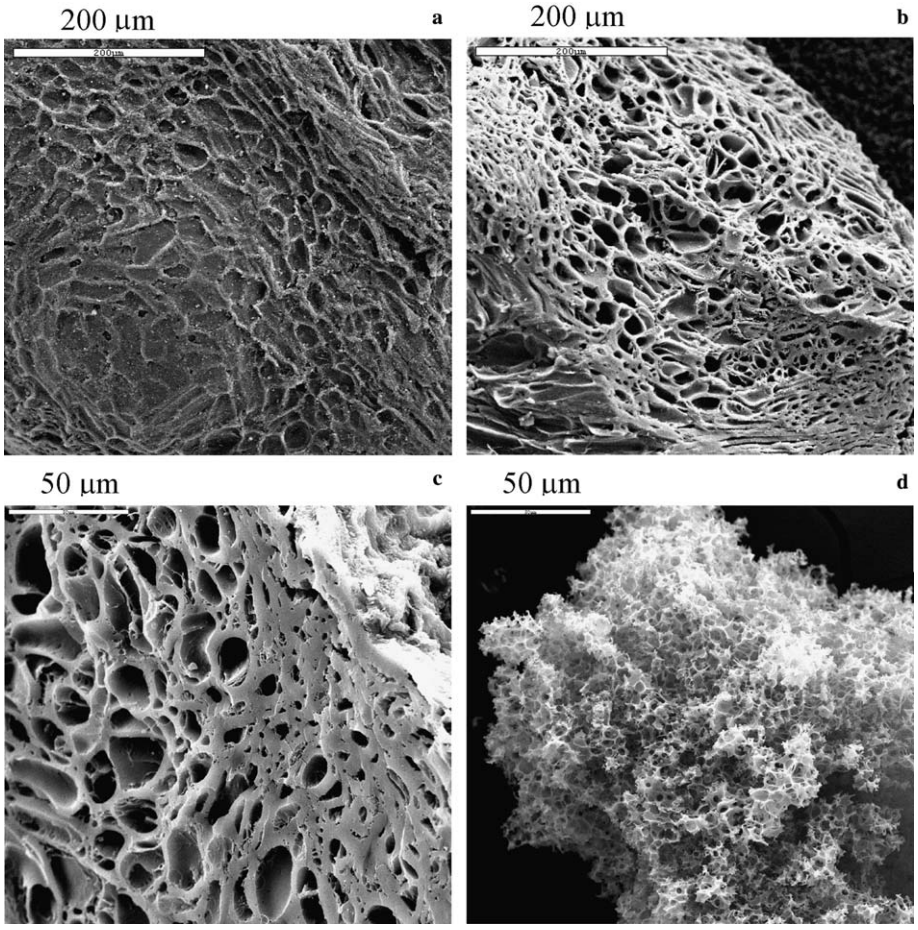

Fig. 5. SEM micrographs of samples: (a) carbonized olive stones; (b) A2; (c) B; (d) H.

(Table 3). When the binder concentration increased from 5% to 15% this micropore volume decreased with regard to sample H. Finally, in all monoliths the $W_0(N_2)$ micropore volume was smaller than in sample H.

Monoliths H-10-5 and H-10-15 were used as adsorbents to remove toluene under dynamic conditions from a toluene/air flow containing 740 ppmv of toluene. A photograph of the column bed used is also shown in Fig. 6. Breakthrough curves obtained are depicted in Fig. 7. Characteristics of the carbon beds were calculated from these curves following a method described elsewhere [29,30] and they are compiled in Table 5. In this table t_B is the breakthrough time, which was taken arbitrarily at a relative concentration of 0.02. X_B is the amount adsorbed at the breakthrough, and X_S is the amount adsorbed at saturation. H_{MTZ} is the height of the mass transfer zone, which is an indication of the rate of adsorbate removal by the adsorbent. The faster the adsorption rate, the lower is the H_{MTZ}. R_{MTZ} is the rate of movement of H_{MTZ}. This parameter depends on the affinity of the adsorbate for the adsorbent and is important for design purposes because it indicates the rate at which the adsorbent will be exhausted. Results displayed in Table 5 indicate that H-10-5 is slightly more effective than H-10-15 in removing toluene under dynamic conditions from a toluene/air flow.

Recently, several authors have reported the adsorption of toluene on different activated carbons; see for instance Ref. [31] and references included there. Thus, Chiang et al. [32] reported toluene adsorption data on activated carbons from different origins and with micropore volumes

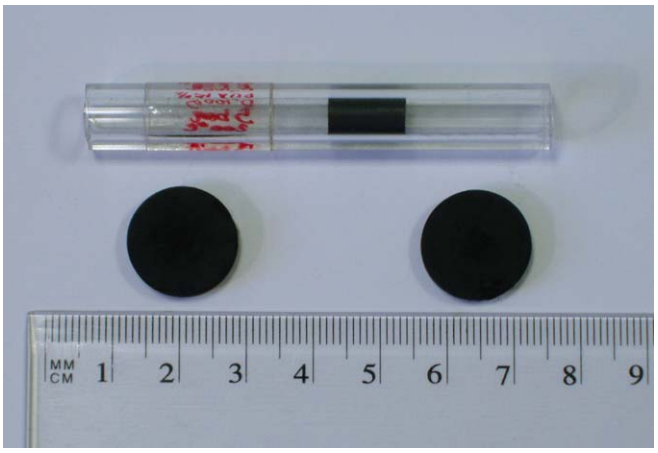

Fig. 6. Activated carbon monoliths.

Table 4
BET surface area and micropore volume, W_0, of different activated carbon monoliths

Monolith	S_{BET} (m^2/g)	$W_0(N_2)$ (cm^3/g)	$W_0(CO_2)$ (cm^3/g)
H-5-5	813	0.48	0.32
H-5-15	775	0.39	0.28
H-10-5	883	0.50	0.34
H-10-15	788	0.40	0.30

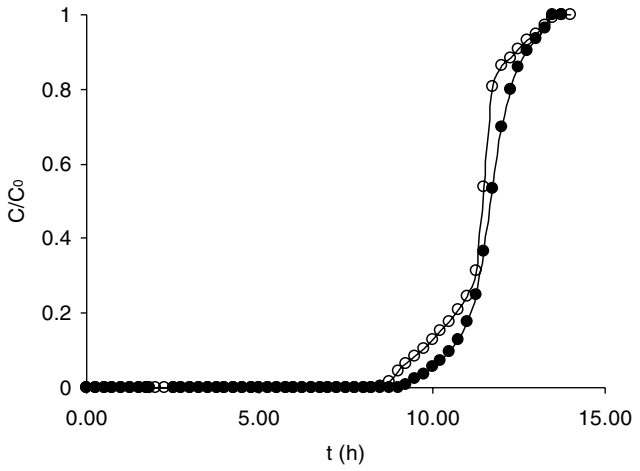

Fig. 7. Toluene breakthrough curves from a toluene/air mixture. (●) H-10-5; (○) H-10-15.

Table 5
Characteristics of the column beds

Monolith	t_B (h)	X_B (g/100 g AC)	X_S (g/100 g AC)	H_{MTZ} (cm)	R_{MTZ} (mm/h)
H-10-5	9.5	60	72	0.22	0.71
H-10-15	8.7	55	70	0.28	0.68

ranging from 0.30 to 0.52 cm^3/g and using an initial toluene concentration of 650 ppmv in N_2, close to that used in the present work. Authors reported toluene adsorption data that varied between 16 and 32 g/100 g AC, which were much lower that those obtained with monolithic activated carbons from olive stones, around 70 g/100 g AC at saturation. Results found are very interesting for the practical application of these monolithic activated carbons for the removal of volatile organic compounds from air.

4. Conclusions

Different activated carbons were obtained by KOH-activation of carbonized olive stones, by changing the KOH/carbon weight ratio and the particle size range of the carbonized olive stones. The best textural characteristics were obtained for a KOH/carbon weight ratio of 2/1 and with particle size range in the raw material between 0.63 and 0.80 mm. This activated carbon was later steam-activated, which produced an increase in the S_{BET} and a widening of micropores.

Other activated carbon was directly prepared by KOH-activation of olive stones. The activated carbon so obtained had a higher S_{BET} and wider microporosity than the same activated carbon obtained from carbonized olive stones. However, it was very light due to the breaking of the olive stone particles after their impregnation with the KOH solution. This was due to the fragmentation and solution of lignin and hemicellulose produced by the attack of strongly nucleophilic hydroxyl ions.

The above carbon was used to manufacture different monoliths by hot pressing a mixture of the activated carbon and polyvinyl alcohol, which acted as a binder. Surface characteristics of monoliths essentially depended on the proportion of binder in the mixture and in a less extent on pressure in the pressure range used. Monoliths were further used to remove toluene from a toluene/air flow. It is noteworthy that the amounts adsorbed at saturation were much higher than others reported in the literature. Results found are very interesting for the practical application of the monolithic activated carbons for the removal of volatile organic compounds from air.

Finally, the present work shows that different granular and powder activated carbons can be obtained by KOH-activation of olive stones and that the latter carbons can be used to prepare monolithic activated carbons.

Acknowledgement

Authors are grateful to MCYT and FEDER, project MAT2001-2874, for financial support.

References

[1] M. Smisek, S. Cerny, Active Carbon: Manufacture, Properties and Applications, Elsevier, Amsterdam, 1970, pp. 10–48.
[2] G.A. Mills, Chemtech 7 (1977) 418.
[3] H. Marsh, P.L. Walker Jr., Fuel Process. Technol. 2 (1979) 61.
[4] H. Marsh, D.S. Yan, T.M. O'Grady, A. Wennerberg, Carbon 22 (1984) 603.
[5] P. Ehrburger, A. Addoun, F. Addoun, J.B. Donnet, Fuel 65 (1986) 1447.

[6] T. Otowa, M. Yamada, R. Tanibata, M. Kawasami, in: E.F. Vansant, R. Dewolfs (Eds.), Gas Separation Technology, Elsevier, Amsterdam, 1990, p. 263.
[7] T. Otowa, R. Tanibata, M. Itoh, Gas. Sep. Purif. 7 (1993) 241.
[8] Z. Hu, E.F. Vansant, Carbon 33 (1995) 1293.
[9] A. Amadpour, D.D. Do, Carbon 34 (1996) 471.
[10] A. Amadpour, D.D. Do, Carbon 35 (1997) 1723.
[11] C. Moreno-Castilla, F. Carrasco-Marín, M.V. López-Ramón, M.A. Álvarez-Merino, Carbon 39 (2001) 1415.
[12] D. Lozano-Castelló, M.A. Lillo-Ródenas, D. Cazorla-Amorós, A. Linares-Solano, Carbon 39 (2001) 741.
[13] M.A. Lillo-Ródenas, D. Lozano-Castelló, D. Cazorla-Amorós, A. Linares-Solano, Carbon 39 (2001) 751.
[14] G.H. Oh, C.R. Park, Fuel 81 (2002) 327.
[15] M.A. Lillo-Ródenas, D. Cazorla-Amorós, A. Linares-Solano, Carbon 41 (2003) 267.
[16] M.A. Lillo-Ródenas, J. Juan-Juan, D. Cazorla-Amorós, A. Linares-Solano, Carbon 42 (2004) 1371.
[17] M. Molina-Sabio, F. Rodríguez-Reinoso, Coll. Surf. A 241 (2004) 15.
[18] R.-L. Tseng, S.-K. Tseng, J. Colloid Interface Sci. 287 (2005) 428.
[19] G.G. Stavropoulos, A.A. Zabaniotou, Micropor. Mesopor. Mater. 82 (2005) 79.
[20] F.-C. Wu, R.-L. Tseng, C.-C. Hu, Micropor. Mesopor. Mater. 80 (2005) 95.
[21] T.L. Cook, C. Komodromos, D.F. Quinn, S. Ragasn, in: T.D. Burchell (Ed.), Carbon Materials for Advanced Technologies, Pergamon, Amsterdam, 1999, pp. 269–302.
[22] F. Derbyshire, M. Jagtoyen, R. Andrews, A. Rao, I. Martín-Gullón, E. Grulke, in: L.R. Radovic (Ed.), Chemistry and Physics of Carbon, vol. 27, Marcel Dekker, New York, 2001, pp. 1–66.
[23] E.S.J. Lox, B.H. Engler, in: G. Ertl, H. Knözinger, J. Weitkamp (Eds.), Environmental Catalysis, Wiley-VCH, Weinheim, 1999, pp. 1–117.
[24] M. Bishop, D.L. Ward, Fuel 37 (1958) 191.
[25] M.V. López-Ramón, C. Moreno-Castilla, J. Rivera-Utrilla, R. Hidalgo-Álvarez, Carbon 31 (1993) 815.
[26] F. Rodríguez-Reinoso, A. Linares-Solano, in: P.A. Thrower (Ed.), Chemistry and Physics of Carbon, vol. 21, Marcel Dekker, New York, 1989, pp. 1–146.
[27] F. Stoeckli, in: J. Patrick (Ed.), Porosity in Carbons, Arnold, London, 1995.
[28] D. Cazorla-Amorós, J. Alcañiz-Monge, M.A. de la Casa-Lillo, A. Linares-Solano, Langmuir 14 (1998) 4589.
[29] J.S. Zogorski, S.D. Faust, in: P.N. Cheremisinoff, F. Ellerbusch (Eds.), Carbon Adsorption Handbook, Ann Arbor Science, Ann Arbor, MI, 1978, pp. 753–777.
[30] M.A. Ferro-García, F. Carrasco-Marín, J. Rivera-Utrilla, E. Utrera-Hidalgo, C. Moreno-Castilla, Carbon 28 (1990) 91.
[31] M.A. Lillo-Ródenas, D. Cazorla-Amorós, A. Linares-Solano, Carbon 43 (2005) 1758.
[32] B.Y.C. Chiang, P.C. Chiang, E.E. Chang, J. Environ. Eng. 127 (2001) 54.